

PAPER • OPEN ACCESS

The Effects of the distance between ground-sill and double cylinder-piers against the scour patterns

To cite this article: M Mera and M Thaahaa 2019 *IOP Conf. Ser.: Mater. Sci. Eng.* **602** 012095

View the [article online](#) for updates and enhancements.

The Effects of the distance between ground-sill and double cylinder-piers against the scour patterns

M Mera¹ and M Thaahaa¹

¹ School of Civil Engineering, Engineering Faculty, the University of Andalas, Kampus Limau Manih, Padang, Indonesia

E-mail: mas_mera@eng.unand.ac.id

Abstract. Flood disaster causes local scouring around the bridge piers. Some efforts to protect piers locally have been widely practiced, but the protective effect is only temporary. This is due to the riverbed being degraded within a few years, and eventually the pier protector is also broken. Ground-sill has a dual function of setting the ground level of the channel and stopping local scouring on the pier to continue. The present study is about physically modelling in the laboratory to observe scour depths due to the distance between the ground-sill and double piers. The position of the double piers remain, *i.e.* a line of flow direction, so there are upstream pier (called pier 1) and downstream pier (called pier 2). Only the ground-sill positions are varied. The ground-sill is located on the downstream of the pier 2. Some experiments are conducted to get the two best positions of the ground-sill by trial and error, that is W_1 (position 1) and W_2 (position 2) using the biggest discharge flow that can be. The position W_1 is better than W_2 . This is based on two criteria: the scour depth has to be stable (no more scour) at the specified time range (0 - 120 minutes), and the maximum scour depth formed has to be the shallowest among those in the other experiments. The resulting two best positions of the ground-sill are then tested with three variations of discharge to observe the scour depth, and to observe the differences of the scour depths due to both piers in point 1 (behind the pier 1), point 2 (right side of the pier 1), point 3 (left side of the pier 1), point 4 (in front of the pier 1), point 5 (behind the pier 2), point 6 (right side of the pier 2), point 7 (left side of the pier 2), and point 8 (in front of the pier 2). The experimental results show that the maximum scour depth with the position W_1 occurs in points 1 and 3 with a 2.9 cm deep and a maximum flow of 3.161 l/s. Meanwhile the maximum scour depth with the position W_2 occurs in point 1 with a 3.8 cm deep and a maximum flow of 3.254 l/s. The scour characteristics with the point W_1 is that a local scouring occurs significantly since the beginning of the flow, but channel bed has been stable since several minutes after the flow starts overtopping the ground-sill. The flow with the position W_2 shows that the backwater affects significantly the flow condition so that scour and sedimentation process continuously occur. This experimentation also confirms that the control slope (the slope between riverbed where the piers are and the top of the ground-sill) has a optimum distance. In this study the optimum control slope is -0.014 .

1. Introduction

By the middle of 2016, 95 percent of disasters happened in Indonesia are hydrometeorology types in which the greatest damage impact occurred is due to flood disaster [1]. During the flood, both riverbed degradation process and local scouring process around the bridge piers can occur simultaneously. In



some cases, the local protection of the bridge piers lasted normally a few years. This was due to the effects of the riverbed degradation [2]. As a result, the protection of the riverbed should be a priority to do. The riverbed protection is usually by building a ground-sill. There are two types of ground-sill, *i.e.*, the bed girdle work is to keep the riverbed does not go down, and the head work is to make the longitudinal slope of riverbed mild.

1.1. Bridge piers

Piers with a cylinder cross-section are commonly used to support a bridge Indonesia. Nowadays, the Indonesian government builds many new long and wide bridges and also builds new long bridges beside the old ones. Consequently the use of double piers can be an alternative [3].

US Department of Transportation reported that bridge pier scour has been studied for more than six decades [4]. Comparative studies of bridge pier scour with other cross-sections have been widely done. One of them was conducted by varying discharge flows. The smallest scours are respectively on piers with the cross section of elliptic and parabolic. The biggest one is on the pier with a rectangular type [5]. The other study was conducted by Ariyanto, *i.e.* by comparing the three types of the piers *i.e.* square, circular and parallelogram using varied discharge flows. The smallest scour is given by the circular one [6]. The other study reported that the types of triangle and square were compared to the circular one respectively increase the backwater 15.5% and 31.5% in the upstream [7].

1.2. Circular pier scour

Scouring mechanism on single-circular pier was specifically analysed by Guo in 2012 by proposing a physically-based scour depth equation for practical design purposes in terms of the pressure gradient through flow-structure, flow-sediment and sediment-structure interactions. The pressure equal is zero at the stagnation point, so that no sediment moves downstream. The maximum pressure gradient occurs at an oblique, so that scour begins at the upstream pier side [8]. Other study regarding scour mechanism was reported by Ashtiani and Kordkandi (2013) for both single and double piers. The results show that the presence of a downstream pier changes the flow structure to a great extent, particularly in the near-wake region [9].

Tippireddy (2017) included the effect of air velocity. Air is injected through a horizontal diffuser pipe. The air injection reduces the local scour at bridge piers in equilibrium conditions by nearly 35%. This scour reduction is caused by a change in flow patterns around the bridge piers with the injection of air bubbles [10]. Pandey *et al* (2017) studied experimentally the variation of temporal scour depth around circular piers under clear-water scour condition for a variability of configuration studies, including different size of circular piers. In front of the pier (0° plane) indicates the maximum and behind the pier (180° plane) indicates minimum scour zones [11].

1.3. Protection against scour

From years to years, pier protection by using ground-sill to control local scouring have been investigated by considering some layouts. One of those studies was conducted in 2011 using ground-sill to protect the piers against scour. This study also included the velocity effects. The result shows that the maximum scour depth at cylinder pier occurred at a speed of 0.267 m/s and the minimum at a speed of 0.157 m/s. At the same flow rate, protection using ground-sill reduces the scour depth to 61.49% [12]. Other study using ground-sill showed that when the level of the spillway as high as that of riverbed, the increase of the flow will deepen the scour. When the level of the spillway is higher than that of pier base, the scour decreases [13].

As a result, in the present study, a physical model is set up using double cylinder-piers and ground-sill with a triangle-spillway. The elevation of the spillway is higher than that of the channel bed where the piers are located to investigate the effects of ground-sill against the characteristics of the local scouring.

2. Materials and method

A physical model is set up as shown in Figure 1.

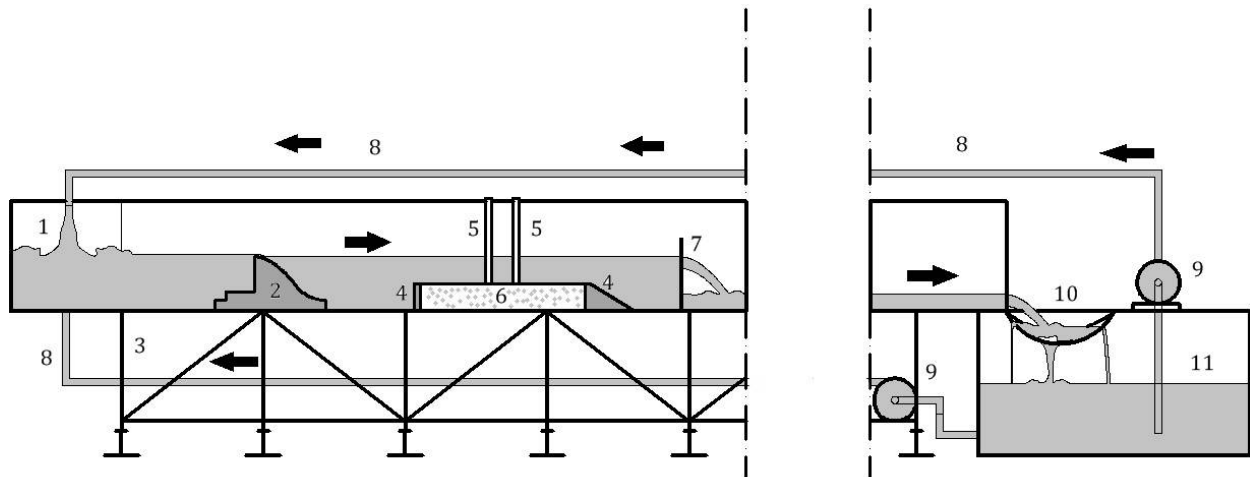


Figure 1. Physical model set-up

2.1. Equipment and materials

The experimentation is run on the rectangular channel with a 12 m length (straight path), a 0.385 m width, and a 0.39 m height. This channel is also equipped by some components as follows:

Stilling basin. Water is pumped to this basin. From this basin, water then flows to the channel.

Ogee-shaped weir

This is a part of the stilling basin to make water still, so that the uniform flow can be obtained.

Metal frame

This is to support and to adjust the longitudinal slope of channel.

Timber wall

This is to increase the level of channel bed and to stop sediment up to a certain level.

Piers

These piers are made of PVC pipe with an outer diameter of 32 mm located in the middle of channel cross-section.

Sand

It is as sediment material.

Sharp-crested weir with a triangle spillway

It is made of acrylic with an angle of 90. This works as a ground-sill.

Pipe

It is to connect water from the receiving basin to the stilling one.

Pump

It is to flow water from the receiving basin to the stilling one.

Filter

It is to trap sediment.

Receiving Basin

A tank to receive water from the channel.

2.2. Method

A physical model of double circular-piers and ground-sill is prepared first. The distance between both piers are three times their diameters as done by Ashtiani and Kordkandi [9]. Both diameters are the same. Other components are positioned as shown in Figure 1. The sediment as base material of the channel bed is determined by following ASTM D854-02 [14]. The sediment is then compacted around both piers. The piers are placed in a flow direction. The distance between the piers and ground-sill is

determined by trial and error using the biggest discharge that can be made the available pumps to fulfil the both criteria. The corresponding criteria are: the scour depth y_s has to be stable (no more scour) at the specified time range (0 to 120 minutes), and the maximum scour depth formed has to be the shallowest among those in the other trials. The rate of discharges are determined by two ways. Firstly, measuring the volume of water that flows within a specified time range. Secondly, using the sharp-crested weir with a triangle spillway [15]. According to Jamal (2007), direct measuring is more accurate than the other method [5]. Each method has advantage and disadvantage. For that reason, the relative error of their differences needs to be checked. The relative error used in the present research is about 0 to 5 %.

Based on the both criteria, take the two best positions of them, *i.e.* W_1 is the first best and W_2 is the second best. The both positions are then observed their effects against scour around the both piers using three varied discharges. The scour depth y_s in observed points are measured from time to time in minutes, *i.e.* at $t = 0, 2, 4, 8, 10, 15, 20, 25, 30, 35, 40, 45, 50, 55, 60, 70, 80, 90, 100, 110$ and 120 for every varied discharge.

Prior to and after running, material samples (sand) on the channel bed is tested using the sieve analysis following ASTM D2478-00 [14] to determine sediment non-uniformity σ . The samples are sand located in the observed points as wide as the diameter of the pier and deeper than the maximum scour depth. After the sieve analysis is done, all sampels are then put back to where they were. The value of sediment non-uniformity σ is determined as [8]

$$\sigma = [D_{84}(D_{16})^{-1}]^{1/2} \quad (1)$$

where D_{84} , D_{50} and D_{16} are the corresponding diameters of 84%, 50% and 16% pass the sieve. The critical velocity U_c is determined using following formula

$$U_c = [K_S (G_S - 1) D_{50} R^{1/3} n^{-2}]^{1/2} \quad (2)$$

where K_S is the parameter Shield and can be determined using the formula

$$K_S = 0.22\beta + 0.06 \cdot 10^{-7.7\beta} \quad (3)$$

$$\beta = \{v^{-1} [(G_S - 1)g(D_{50})^3]^{1/2}\}^{-0.6} \quad (4)$$

in which v is the kinematic viscosity, G_S is the specific gravity, g is the gravitation acceleration. The Manning coefficient n is determined as

$$n = 0.041(D_{50})^{1/6} \quad (5)$$

3. Results and discussions

The present study can be divided by two types, *i.e.* to vary the position of the ground-sill and to vary the discharge flows.

3.1. Ground-sill positions

The experimentation about varied positions of the ground-sill is to determine the best distance of the ground-sill from the piers. This is obtained after three runs with the biggest discharge that can be. The

first run, the ground-sill is positioned about 155.2 cm far from the centre of the double piers. This gives maximum scour depth $y_{s-max} = -3.8$ cm. This depth is unstable within 120 minute run. The second run, the ground-sill is moved 50 cm downward to 205.2 cm far from the centre of the piers. This gives maximum scour depth $y_{s-max} = -4$ cm. This depth is also unstable within 120 minute run. The last run, the ground-sill is moved 50 cm downward again to 255.2 cm far from the centre of the piers. This gives maximum scour depth $y_{s-max} = -3$ cm. This depth has been stable since 70 minute run. From the three runs gives the first position W_1 is 252.2 cm far from the centre of the piers with $y_{s-max} = -3$ cm, and the second position W_2 is 155.2 cm far from the centre of the piers $y_{s-max} = -3.8$ cm.

3.2. Determination of discharge flows

Once the positions of ground-sill are determined, *i.e.* W_1 and W_2 , the next runs are to vary discharge flows. As a result, the rate of discharge then has to be determined. The determination of the flow rate uses a triangle-shaped weir following SNI 8137: 2015 [15]. These results are then compared to the direct measurements as shown in Table 1. From the comparison can be seen that the relative errors are tolerable. As a result, the results based on the direct measurement method are then used.

Table 1. Comparison of the flow rates determined by both the direct measurements and triangle-sharp weir methods.

No	Variations	Flow Rate Q (l/s)		Relative error (%)
		Determined by methods		
		Direct measurement	Triangle-shaped weir	
1	W1Q1	0.842	0.842	0.00
2	W1Q2	1.590	1.586	0.25
3	W1Q3	3.161	3.157	0.13
4	W2Q1	0.969	0.968	0.10
5	W2Q2	1.528	1.527	0.07
6	W2Q3	3.254	3.247	0.22

Table 2. Calculation to indicate scour by assessing Froude number F close to 1 and $U_0/U_c \geq 1$

Variation	Pier	Condition	h (cm)	A (cm ²)	U_0 (m/s)	F	σ	D_{50} (mm)	K_s	U_c (m/s)	$\frac{U_0}{U_c}$
W1Q1	1	Starting	0.8	30.80	0,273	0,975	2.081	0.392	0.033	0.181	1.507
		Ending	10.2	392.70	0,021	0,021	2.386	0.368	0.034	0.263	0.082
	2	Starting	0.8	30.80	0,273	0,975	2.182	0.373	0.034	0.183	1.496
		Ending	10.2	392.70	0,021	0,021	2.338	0.403	0.060	0.348	0.062
W1Q2	1	Starting	1.3	50.05	0,318	0,890	2.112	0.373	0.034	0.194	1.637
		Ending	11.7	450.45	0,035	0,033	3.330	0.417	0.033	0.257	0.137
	2	Starting	1.3	50.05	0,318	0,890	2.169	0.409	0.033	0.191	1.659
		Ending	11.7	450.45	0,035	0,033	2.302	0.381	0.034	0.260	0.136
W1Q3	1	Starting	2.0	77.00	0,411	0,927	2.134	0.393	0.033	0.209	1.961
		Ending	13.8	531.30	0,059	0,051	3.450	0.413	0.033	0.267	0.223
	2	Starting	2.0	77.00	0,411	0,927	2.089	0.423	0.033	0.207	1.980
		Ending	13.8	531.30	0,059	0,051	2.241	0.458	0.032	0.264	0.225
W2Q1	1	Starting	0.9	34.65	0.280	0.941	2.238	0.393	0.033	0.185	1.513
		Ending	9.0	346.50	0.028	0.030	2.378	0.413	0.033	0.255	0.110
	2	Starting	0.9	34.65	0.280	0.941	2.302	0.423	0.033	0.183	1.527
		Ending	9.0	346.50	0.028	0.030	2.353	0.458	0.032	0.252	0.111
W2Q2	1	Starting	1.2	46.20	0.331	0.964	2.279	0.398	0.033	0.194	1.705
		Ending	10.1	388.85	0.039	0.039	2.574	0.451	0.032	0.257	0.153
	2	Starting	1.2	46.20	0.331	0.964	2.507	0.394	0.033	0.194	1.703
		Ending	10.1	388.85	0.039	0.039	2.401	0.416	0.033	0.259	0.152
W2Q3	1	Starting	2.0	77.00	0.423	0.954	2.576	0.398	0.033	0.210	2.014
		Ending	12.4	477.40	0.068	0.062	3.050	0.451	0.032	0.263	0.260
	2	Starting	2.0	77.00	0.423	0.954	2.200	0.394	0.033	0.210	2.011
		Ending	12.4	477.40	0.068	0.062	2.187	0.416	0.033	0.265	0.258

3.3. Sediment movement with varied discharge flows

Based on measurements are obtained as follows the specific gravity G_s is 2.565, water temperature T is 26°C. Based on the given T , then the kinematic viscosity ν is 8.729×10^{-7} m²/s. Table 2 shows the calculation to indicate the scour can occur if the Froude number F is close to 1 [8] and U_0/U_c is equal or bigger than 1 [16]. W1Q1 is the weir or ground-sill in position 1 with the smallest discharge, Pier 1 is the pier located in the upstream, Pier 2 is in the downstream, h is water depth, A is the wet area equal to h times b , U_0 is the incident flow, F is the Froude number, σ is sediment non-uniformity, D_{50} is the corresponding diameters of 50% pass the sieve, K_s is the parameter Shield, U_c is the critical velocity.

3.4. Scour depth against time with varied flows in the layouts W_1 and W_2

Scour in the observed point 1 (behind the pier 1). Figures 2 and 3 show that the scouring process significantly occurs in minutes 0 to 2 in the (observed) point 1. After that scouring and sedimentation take place in turn up to certain minutes. The increase of the flow rate will deepen scour. The phenomena are similar to both weir positions. The maximum scour depth at the position W_1 v_{s-max} is 2.9 cm with Q_3 (the biggest flow) and at W_2 is 3.8 cm with Q_3 .

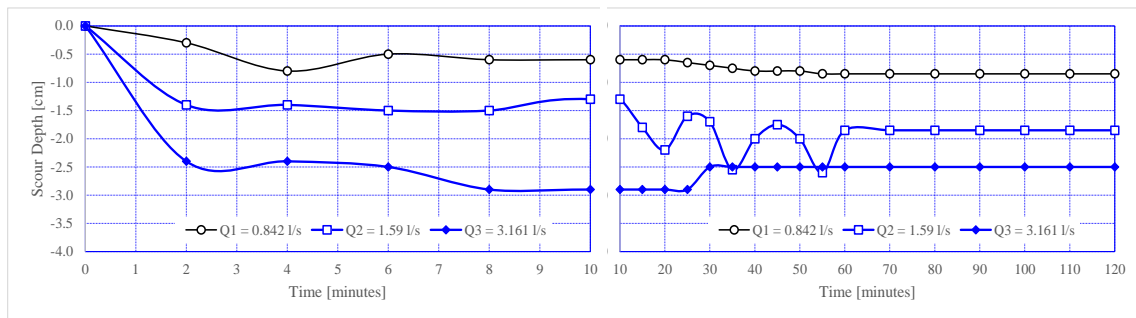


Figure 2. Observed point 1: scour depth and against time with varied flows in the position W_1 in 0 to 120 minutes

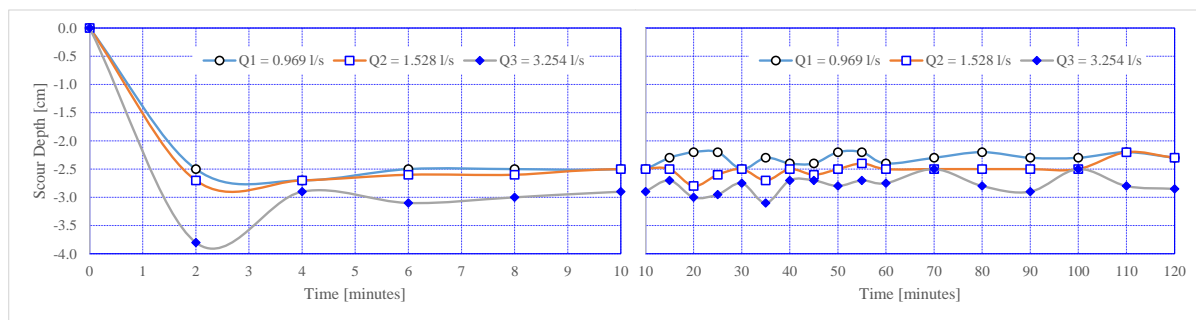


Figure 3. Observed point 1: scour depth and against time with varied flows in the position W_2 in 0 to 120 minutes

Scour in the observed point 2 (right side of the pier 1). The same phenomena as in the point 1 also occur in the point 2 for both ground-sill positions, *i.e.* the scouring process significantly occurs in minutes 0 to 2. After that scouring and sedimentation take place in turn up to certain minutes. The increase of the flow rate will deepen scour. All are shown in Figures 4 and 5.

Scour in the observed point 3 (left side of the pier 1). Figures 6 and 7 show similar phenomena as those in the previous points. The maximum scour depth y_{s-max} is 2.9 cm with Q_3 at the position W_1 .

Scour in the observed point 4 (in front of the pier 1). Figure 8 shows the phenomena in the point 4 with the position W_1 , in which the scouring process significantly occurs in minutes 0 to 2. Scouring due to Q_2 is more worse than that due to Q_3 . The next minutes, scouring and sedimentation take place in turn up to certain minutes. The variation due to Q_3 reaches the stability first. In this observed point, the increasing of flow doesn't deepen the scouring. The maximum scour depth occurs in the minutes 45 due to Q_2 . Figure 9 shows that the phenomena in the observed point 4 with the position W_2 , in which the scouring process significantly occurs in minutes 0 to 2. From 2 to 120 minutes, scouring and sedimentation take place in turn. In here, the increasing of flow will deepen the scour.

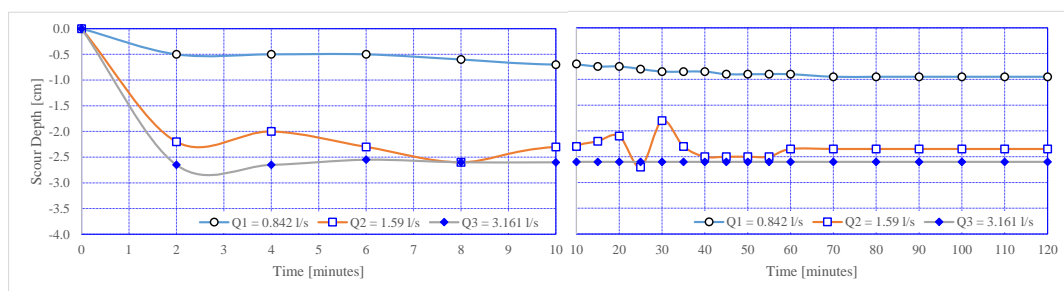


Figure 4. Observed point 2: scour depth and against time with varied flows in the position W_1 in 0 to 120 minutes.

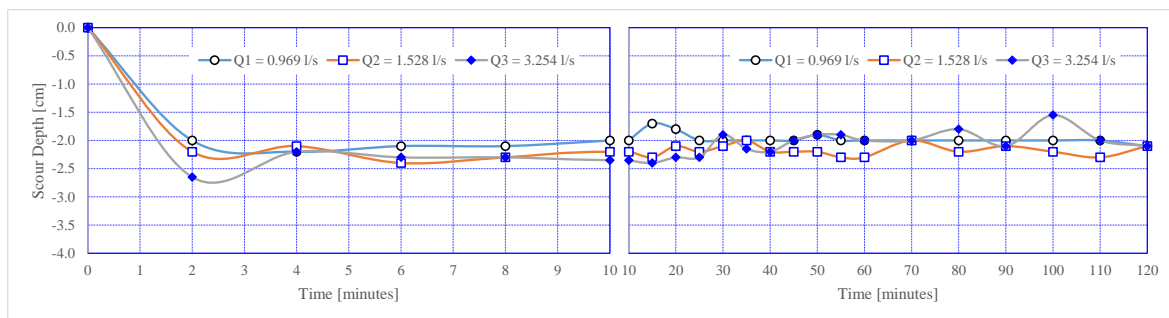


Figure 5. Observed point 2: scour depth and against time with varied flows in the position W_2 in 0 to 120 minutes.

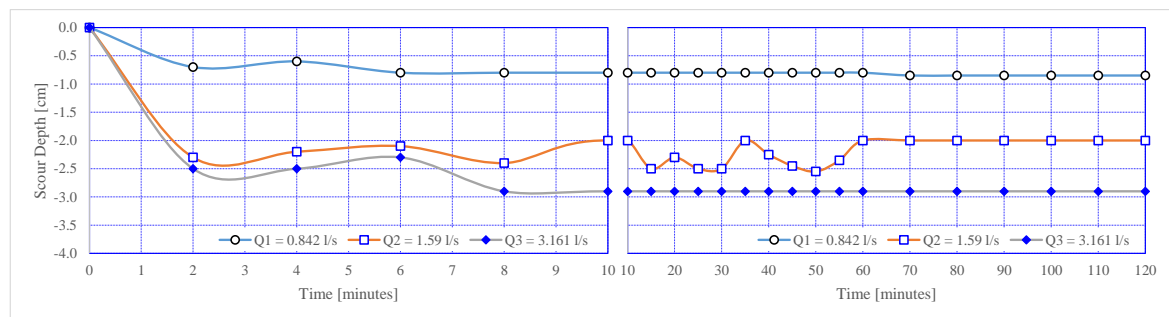


Figure 6. Observed point 3: scour depth and against time with varied flows in the position W_1 in 0 to 120 minutes.

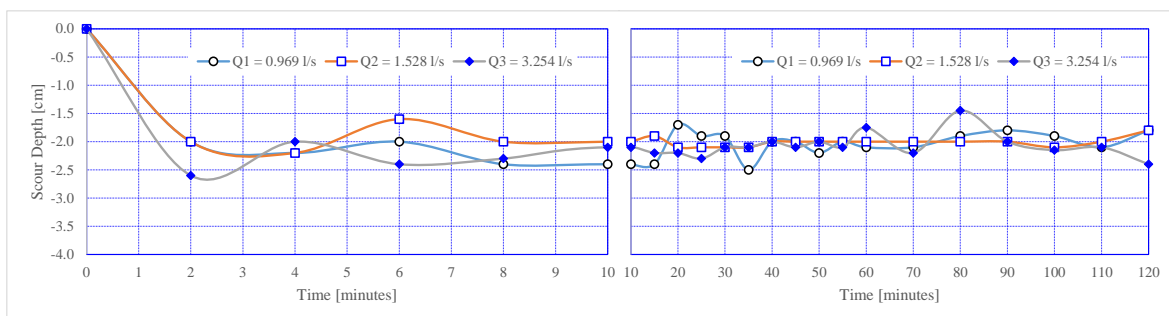


Figure 7. Observed point 3: scour depth and against time with varied flows in the position W_2 in 0 to 120 minutes

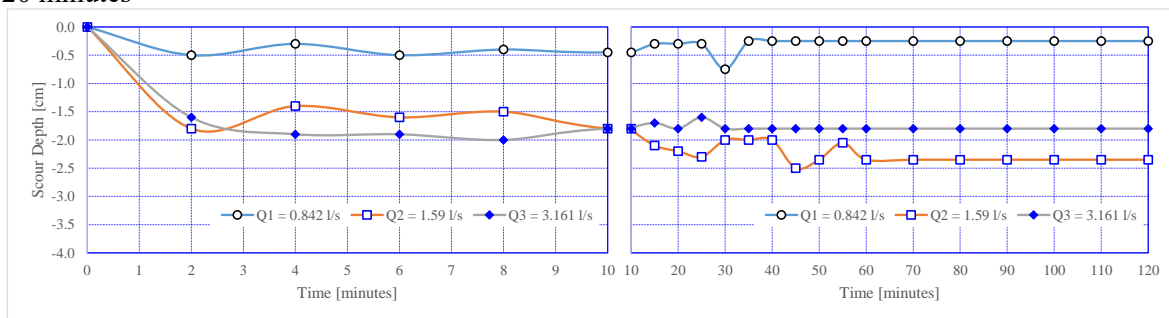


Figure 8. Observed point 4: scour depth and against time with varied flows in the position W_1 in 0 to 120 minutes.

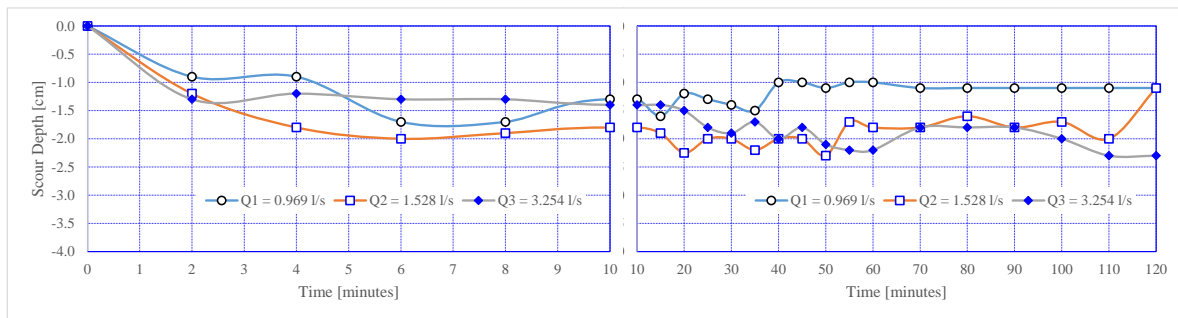


Figure 9. Observed point 4: scour depth and against time with varied flows in the position W_2 in 0 to 120 minutes.

Scour in the observed point 5 (behind of the pier 2). From Figure 10 can be seen that in the position W_1 , the scouring process significantly occurs in minutes 0 to 2 in which the scour due to Q_2 is deeper than that due to Q_3 . As in the previous points, scouring and sedimentation take place in turn in the next minutes. In the minutes 45, the stability is reached for all varied flows. Figure 11 shows that the phenomena happening in the position W_1 are also happening in W_2 for point 5.

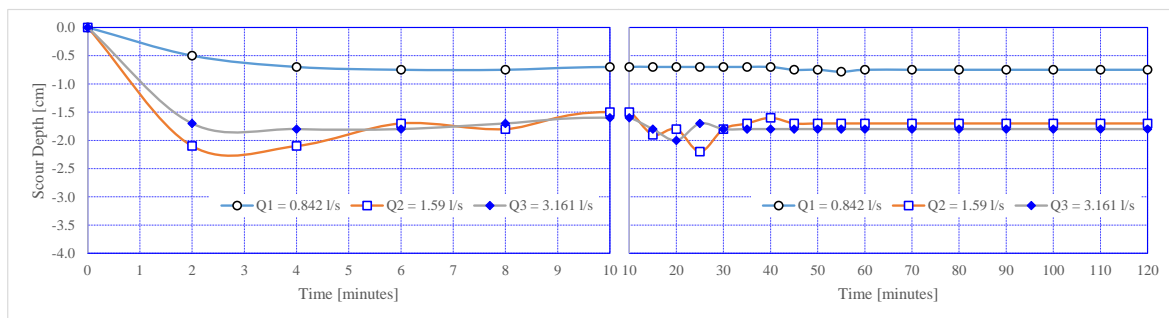


Figure 10. Observed point 5: scour depth and against time with varied flows in the position W_1 in 0 to 120 minutes

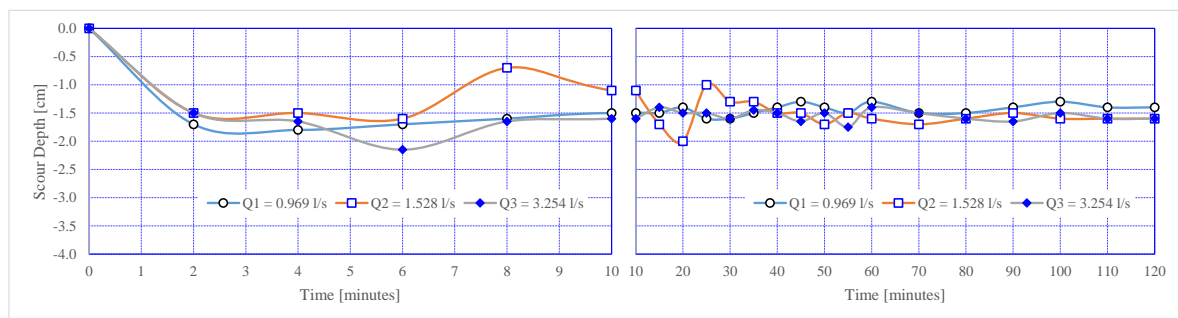


Figure 11. Observed point 5: scour depth and against time with varied flows in the position W_2 in 0 to 120 minutes

Scour in the observed point 6 (right side of the pier 2). Figures 12 and 13 show the same phenomena for both positions in which the scouring process significantly occurs in minutes 0 to 2. Then, scouring and sedimentation take place in turn in the next minutes.

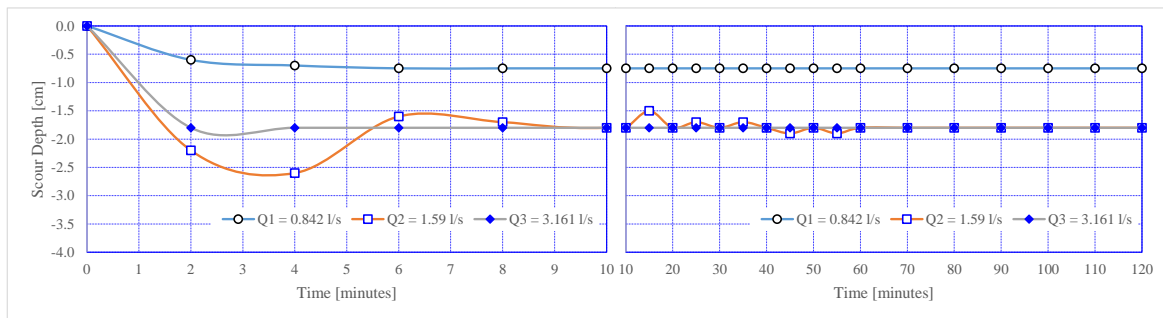


Figure 12. Observed point 6: scour depth and against time with varied flows in the position W_1 in 0 to 120 minutes.

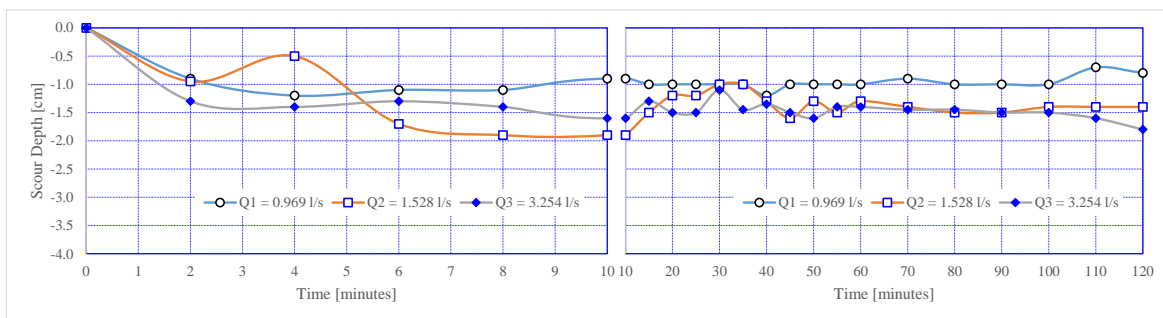


Figure 13. Observed point 6: scour depth and against time with varied flows in the position W_2 in 0 to 120 minutes.

Scour in the observed point 7 (left side of the pier 2). Phenomena in the point 7 are similar to those in the point 6 for both positions. They all can be seen in Figures 14 and 15.

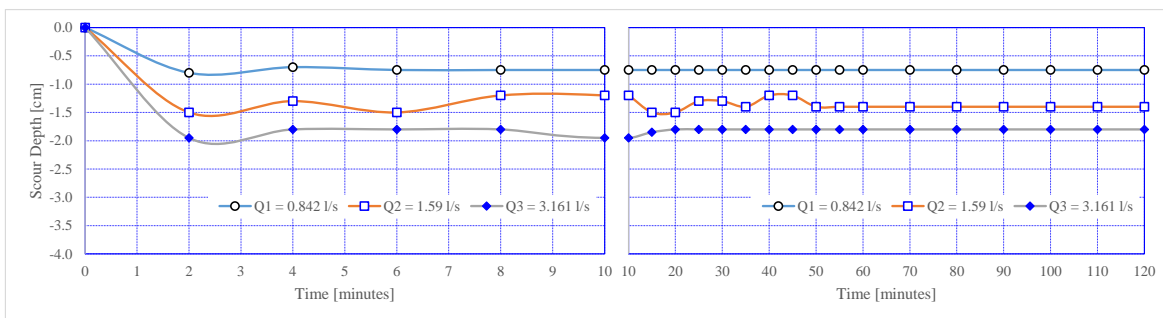


Figure 14. Observed point 7: scour depth and against time with varied flows in the position W_1 in 0 to 120 minutes.

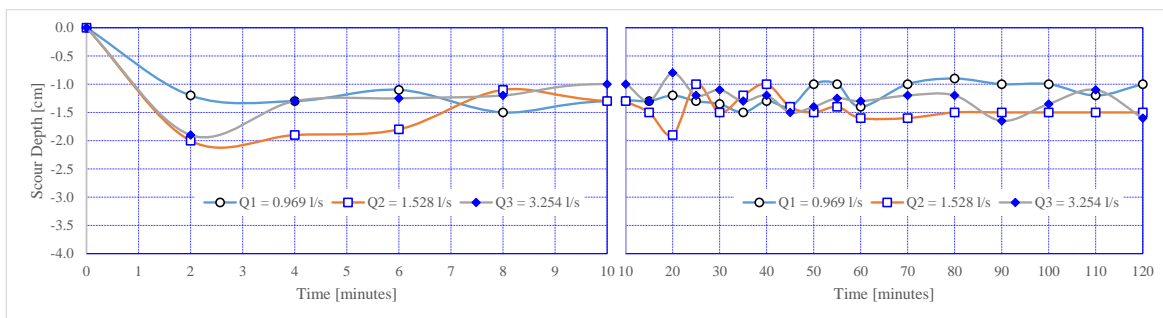


Figure 15. Observed point 7: scour depth and against time with varied flows in the position W_2 in 0 to 120 minutes.

Scour in the observed point 8 (in front of the pier 2). In the ground-sill position 1, phenomena in the observed point 8 are similar to those in the point 7, the scouring process significantly occurs in minutes 0 to 2 (Figure 16). However, in the position 2, the scouring process significant only occur due to Q_3 . The maximum scour depth occur in minutes 60 and 80 (Figure 17).

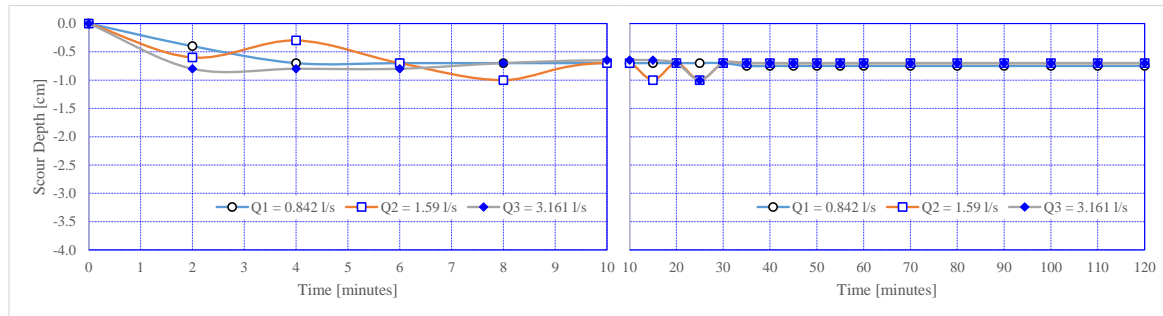


Figure 16. Observed point 8: scour depth and against time with varied flows in the position W_1 in 0 to 120 minutes

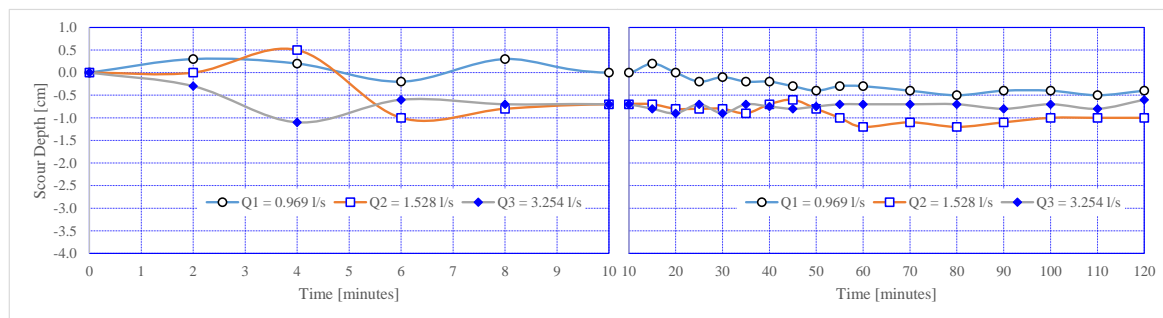


Figure 17. Observed point 8: scour depth and against time with varied flows in the position W_2 in 0 to 120 minutes

More discussions. As seen from Figures 2 to 16, mostly scour occurs significantly in minutes 0 to 2. This is due to the incoming flow has not been restrained by the ground-sill yet. As a result, the flow-structures like down-flow, horseshoe vortex and shedding vortex have not been formed completely [9]. Since the minutes 4, the flow has overtopped the ground-sill crest, so that the flow-structure, flow-sediment and sediment-structure interaction have been completely formed [8].

If it is related to Table 2, when the flow is overtopping the weir crest with the position W_1 , scour and sedimentation processes occur at every point are mostly affected by the biggest flows and also affected by the formation of the three flow-structures. In this configuration, the backwater due to the ground-sill doesn't significantly affect the scour and sedimentation. This is confirmed that a few minutes after overtopping, all phenomena of the scour and sedimentation reduce significantly. The flow profile in a vertical way is nearly flat and the flow overtops in the same elevation on the top of weir crest.

Meanwhile in the position W_2 , scour and sedimentation around the piers occurs to take place in turn. The backwater still affects the flow profile and followed by the pressure gradient, so that the flow-structure still varies [17].

As seen in Table 2 with the position W_1 , in every Q , the values σ on upstream pier and downstream pier always increase. This indicates the sediment around them become more non-uniform. This is due to the process of armouring layer has been formed and can be seen visually in Figure 18 (left) in which the larger grains accumulate around the piers. The velocity is not big enough to scour because $U_0/U_c < 0,4$.

However, in the position W_2 , the values σ on upstream and downstream piers increase for Q_1 (i.e. W2Q1), but for Q_2 (i.e. W2Q2) and Q_3 (i.e. W2Q3), they decrease on downstream piers and increase

on upstream piers. It can be seen visually in Figure 18 (right). This indicates that sedimentation around the downstream piers with W2Q2 and W2Q3 is getting more uniform and $U_0/U_c < 0,4$ is not strong enough to scour.



Figure 18. Holes due to scour, and armouring layers around the piers in the position W_1 (left figure) and in the position W_2 (right figure)

The critical slope i_c for the position W_1 is -0.014 (measured) in range -0.011 to -0.022 as recommended [13] and $i_c = -0.023$ for the position W_2 not in recommended range. As a result, it can be said that the position W_1 shows scour mechanism on piers with the optimally protected condition and the position W_2 shows scour mechanism on piers with the optimally less-protected condition.

4. Conclusions

The existence of a ground-sill on the downstream of double circular-piers will reduce the scour depth significantly when the flow overtop the spillway. The elevation of the spillway should be higher than that of pier base. In the best position of the ground-sill (W_1), when the flow rate increases, the maxima scour depths occur on behind (observed point 1), right (point 2) and left (point 3) sides of upstream pier and the stability will reach shortly. Meanwhile in the second best position W_2 , when the flow rate increases, the maxima scour depths occur on behind (point 1), right (point 2), left (point 3) sides and in front of (point 4) upstream pier. In the position W_1 , the maxima scour depths are 2.9 cm (in points 1 and 3) with $Q_3 = 3.161$ l/s. In the position W_2 , the maximum scour depth is 3.8 cm (in point 1) with $Q_3 = 3.254$ l/s.

Restraining the flow using a ground-sill should have a critical slope in recommended range. In the present study, the critical slope i_c is -0.014 .

Acknowledgements

The present work is done experimentally in the Laboratory of Fluid Mechanics and Hydraulics, and in Laboratory of Soil Mechanics. Both laboratories are in the School of Civil Engineering, Faculty of Engineering, the University of Andalas. The present authors thank to all students who work in both laboratories. We also thank to the School of Civil Engineering and Faculty of Engineering, the University of Andalas for supporting this publication (seminar registration).

References

- [1] Kompas 2016 *Potensi Bencana Kian Tinggi* 1 [in Indonesian]
- [2] Istiarto 2009 Bridge Pier Protection Against Riverbed Protection *Proc. ACEC'01*
- [3] Ettema R, Constantinescu G, Melville B W 2017 Flow-Field Complexity and Design Estimation of Pier-Scour Depth: Sixty Years since Laursen and Toch *Journal of Hydraulic Engineering* **143** 1–14

- [4] Guo J, Suaznabar O, Shan H, Shen J 2012 *Pier Scour in Clear-Water Condition with Non-Uniform Bed Materials* TFHRC, McLean, VA, Tech. Rep. FHWA-HRT-12-022
- [5] Jamal R 2007 Studi Pengaruh Bentuk Geometris Bangunan Penghalang Terhadap Gejala Gerusan Setempat (Local Scouring) Yang Terjadi Pada Saluran Yang Lurus *Bachelor Thesis of Andalas University* [in Indonesian]
- [6] Ariyanto A 2009 Analisis Bentuk Pilar Jembatan Terhadap Potensi Gerusan Lokal (Model Pilar Berpenampang Bujur Sangkar, Bulat dan Jajaran Genjang) *Jurnal APTEK* **1** 41–51 [in Indonesian]
- [7] Mohammed M I I, Eid M A A H 2016 Effect of Erodible Bed on Backwater Rise Due to Bridge Piers Only In Case of Subcritical Flow *American Journal of Engineering and Technology Research* **16** 21–34
- [8] Guo J 2012 Pier Scour in Clear Water For Sediment Mixtures *Journal of Hydraulic Research* **50** 18–27
- [9] Ataie-Ashtiani B, Aslani-Kordkandi A 2013 Flow Field Around Single and Tandem Piers *Flow, Turbulence and Combustion* **471** 471–490
- [10] Tippireddy R T R 2017 Air Injecton as a Scour Countermeasure at Bridge Piers *Master Thesis of Michigan Technological University*
- [11] Pandey M, Sharma P K, Ahmad Z, Singh U K 2017 Experimental investigation of clear-water temporal scour variation around bridge pier in gravel *Environmental Fluid Mechanics* **13** 1–20
- [12] Sucipto 2011 Pengaruh Kecepatan Aliran Terhadap Gerusan Lokal Pada Pilar Jembatan Dengan Perlindungan Groundsill *Jurnal Teknik Sipil Perencanaan* **13** 51–56 [in Indonesian]
- [13] Sun D P, Wang L S, Wang P T 2012 Study on the local scouring of the bridge with sediment control dam *Applied Mechanics and Materials* **204-208** 2230–2235
- [14] LMT 2013 *Penuntun Praktikum Mekanika Tanah*, Laboratorium Mekanika Tanah Fakultas Teknik Universitas Andalas [in Indonesian]
- [15] SNI 2015 *Pengukuran Debit Pada Saluran Terbuka Menggunakan Bangunan Tipe Pelimpah Atas* SNI 8137:2015 [in Indonesian]
- [16] Arneson L A, Zevenbergen L W, Lagasse P F, Clopper P E 2012 *Evaluating Scour at Bridges, Fifth Edition*, FHWA, Springfield, VA, Tech. Rep. FHWA-HIF-12-003.
- [17] Hidayat H, Vermeulen B, Sassi M, Torfs P J J F, Hoitink A J F 2011 Discharge Estimation in a Backwater Affected Meandering River *Flow, Hydrology and Earth System Sciences* **15** 2717–2728